Genomics 96 (2010) 57–65

Contents lists available at ScienceDirect

Genomics

journal homepage: www.elsevier.com/locate/ygeno

Investigation of low-dose ritonavir on human peripheral blood mononuclear cells using gene expression whole genome microarrays

Saliha Yilmaz [a,*], Marta Boffito [b], Sophie Collot-Teixeira [a], Ferruccio De Lorenzo [c], Laura Waters [b], Carl Fletcher [b], David Back [d], Anton Pozniak [b], Brian Gazzard [b], John Louis McGregor [a,e]

[a] Cardiovascular Division, King's College London, London, UK
[b] St. Stephen AIDS Trust, Chelsea and Westminster Hospital NHS Foundation Trust, London, UK
[c] Beta Cell Diabetes Centre, Chelsea and Westminster Hospital NHS Foundation Trust, London, UK
[d] Department of Pharmacology, University of Liverpool, Liverpool, UK
[e] INSERM U970, PARC Hôpital Européen George Pompidou Paris, France

ARTICLE INFO

Article history:
Received 1 December 2009
Accepted 23 March 2010
Available online 28 March 2010

Keywords:
PBMC
Ritonavir
Gene expression microarray
Bioinformatics
Biomarker

ABSTRACT

Ritonavir is a protease inhibitor associated with metabolic abnormalities and cardiovascular disease. We have investigated the effects of low-dose ritonavir treatment on gene expression in peripheral blood mononuclear cells (PBMC) of 10 healthy donors. Results using whole genome Illumina microarrays show that ritonavir modulates a number of genes implicated in lipid metabolism, inflammation and atherosclerosis. These candidate genes are dual specificity phosphatase 1 DUSP1), Kelch domain containing 3 (KLHDC3), neutral cholesterol ester hydrolase 1 (NCEH1) and acyl-CoA synthetase short-chain family member 2 (ACSS2). Validation experiments using quantitative PCR showed that ritonavir (at 100 mg once daily and 100 mg twice daily significantly down-regulated these 4 selected candidate genes in 20 healthy individuals. Lower expression levels of these 4 candidate genes, known to play a critical role in inflammation, lipid metabolism and atherosclerosis, may explain ritonavir adverse effects in patients.

Introduction

In the treatment of Human immunodeficiency virus (HIV) infected patients, protease inhibitors (PI) inhibit catalytic activity of HIV aspartyl protease leading to the production of immature, non-functional viral particles. There are currently 10 approved PI used for HIV therapy [1]. The PI ritonavir, initially prescribed at therapeutic doses (600 mg twice daily), was associated with important side effects [2]. It is nowadays used at lower doses (e.g. 100 mg once or twice daily) as a pharmacokinetic (PK) booster in combination with a second PI [3]. Administration of therapeutic doses of ritonavir has been associated with metabolic abnormalities and cardiovascular disease [4]. Also, low-dose ritonavir has been shown to increase cholesterol, low-density lipoprotein (LDL) triglycerides and to decrease high-density lipoprotein (HDL) over 2 weeks in healthy volunteers [5,6]. Due to the complexity of interactions and number of pathways implicated, the causes and mechanisms are still unclear. Moreover, it is not clear if HIV infection *per se* is implicated in some of side effects experienced by HIV-infected individuals on antiretroviral therapy.

Gene expression studies, using whole genome microarrays in tandem with bioinformatics and validation by real time quantitative PCR (Q-PCR) are increasingly being used in investigating vascular, inflammatory, metabolic diseases and the pharmacogenomics of therapeutic drugs. The molecular effects of ritonavir has been investigated on 3T3-L1 murine adipocytes [7,8], human osteoblast [9], human hepatocytes [8] and on murine liver [10]. However, very little is yet known on the role and/or action of ritonavir. In this study, we have investigated using whole genome Illumina microarrays, the effects of low-dose ritonavir treatment on peripheral blood mononuclear cells (PBMC) of 10 healthy donors. Results have allowed us to identify differentially expressed genes and affected biological function pathways.

Results

Microarrays data were analysed to identify candidate genes using 3 different algorithms. Moreover, functional class scoring was performed to identify alterations in key cellular functions induced by ritonavir. Selected candidates genes were further validated by Q-PCR. Pathway analysis was performed to identify genes that link the validated candidate genes.

Candidate genes

Normalised microarray data were analysed by using three different algorithms (Random-variance *t*-test, SAM and ANOVA). Each of the three algorithms gave a list of significantly modulated

* Corresponding author. Cardiovascular Division, King's College London, 3.38 Franklin-Wilkins Building, 150 Stamford Street, London SE1 9NH, UK. Fax: +44 020 7848 3743.
E-mail address: saliha.yilmaz@kcl.ac.uk (S. Yilmaz).

0888-7543/$ – see front matter © 2010 Elsevier Inc. All rights reserved.
doi:10.1016/j.ygeno.2010.03.011

Table 1
Thirty six candidate genes modulated in PBMC by ritonavir.

Gene symbol	Genes description	Parametric *p*-value	Permutation *p*-value	Intensities ratio (AT/BT)	Function summary (Goterms or/and SP_PIR _KEYWORDS)
NCEH1	neutral cholesterol ester hydrolase 1	0.001	0.004	0.89	Lipid metabolism. GO: - Cholesterol ester hydrolase - Lipid catabolic process - Endoplasmic reticulum
ACSS2	Acyl-CoA synthetase short-chain family member 2	0.001	0.004	0.86	Lipid metabolism, Golgi apparatus. Synthesis of cholesterol and unsaturated fatty acids. Glycolysis/gluconeogenesis pathway. GO: - Protein binding - Nucleotide binding - Lipid biosynthetic process - Nucleus
ANKRD17	Ankyrin repeat domain 17	0.001	0.002	0.95	Response to stress
AP1M1	Adaptor-related protein complex 1, mu 1 subunit	0.000	0.002	0.83	Medium chain of the trans-Golgi network clathrin-associated protein complex AP-1. Golgi apparatus. HIV-1 protein interactions with this gene that is involved in HIV infection. GO: - Protein binding - Intracellular protein transport - Golgi apparatus
AQR	Aquarius homolog	0.001	0.002	0.94	Nucleobase, nucleoside, nucleotide and nucleic acid metabolic process, nucleic acid binding. GO: - RNA binding - mRNA processing - Spliceosomal complex
ARHGAP1	Rho GTPase activating protein 1	0.000	0.002	0.86	D4-GDI signalling pathway, Erk and PI-3 kinase. Immunology. GO: - Protein binding, GTPase activator activity - Regulation of GTPase activity - Plasma membrane
ASF1B	ASF1 anti-silencing function 1 homolog B	0.001	0.002	0.93	Modulating the nucleosome structure of chromatin. Efficiency of nucleosome assembly. GO: - Histone binding - Chromatin assembly or disassembly, nucleosome assembly - Chromatin
FAM110A	Family with sequence similarity 110, member A	0.001	0.002	0.79	GO: - Protein binding - Centrosome
C2CD2	C2 calcium-dependent domain containing 2	0.000	0.002	0.89	
CTDSP2	CTD (carboxy-terminal domain, RNA polymerase II, polypeptide A) small phosphatase 2	0.001	0.002	0.76	Promoter clearance during steroid-activated transcription. GO: - Hydrolase activity
DUSP1	Dual specificity phosphatase 1	0.001	0.004	0.73	Response to stress. Non-receptor-type protein-tyrosine phosphatase family. Phosphatase activity, inactivates mitogen-activated protein (MAP) kinase. GO: - MAP kinase tyrosine/serine/threonine phosphatase activity - Intracellular signalling cascade, response to oxidative stress

ERCC1	Excision repair cross-complementing rodent repair deficiency, complementation group 1	0.0000	0.0020	0.93	Response to stress. Human DNA repair gene. GO: - Hydrolase activity, damaged DNA binding - Response to oxidative stress, response to DNA damage stimulus - Nuclear chromosome, telomeric region
ETV6	Ets variant gene 6 (TEL oncogene)	0.0001	0.0020	0.86	Hematopoiesis and maintenance of the developing vascular network. GO: - Protein domain specific binding, sequence-specific DNA binding - Regulation of transcription, DNA-dependent - Nucleus
DEF8	Differentially expressed in FDCP 8 homolog	0.0006	0.0039	0.87	GO: - Diacylglycerol binding, zinc ion binding - Intracellular signalling cascade
GALE	UDP-galactose-4-epimerase	0.0006	0.0020	0.92	Galactose pathway. Synthesis of glycoproteins and glycolipids. GO: - UDP-glucose-4-epimerase activity - Galactose catabolic process
HCFC1	Host cell factor C1	0.0006	0.0020	0.83	Involved in control of the cell cycle and transcriptional regulation during herpes simplex virus infection. GO: - Transcription coactivator activity positive regulation of cell cycle - Nucleus
HPS6	Hermansky–Pudlak syndrome 6	0.0005	0.0020	0.84	GO: - Protein binding - Blood coagulation, melanocyte differentiation, pigmentation
KIAA0513	KIAA0513	0.0001	0.0020	0.83	
KLHDC3	Kelch domain containing 3	0.0001	0.0020	0.85	GO: - Chromatin binding - Reciprocal meiotic recombination - Nuclear chromatin
TMEM179B	Transmembrane protein 179B	0.0002	0.0039	0.89	GO: - Integral to membrane
MAP3K6	Mitogen-activated protein kinase kinase kinase 6	0.0006	0.0020	0.90	Stress-activated protein kinase signalling pathway. MAPK signalling pathway. GO: -Protein serine/threonine kinase activity, nucleotide binding -Activation of JUN kinase activity
NFXL1	Nuclear transcription factor, X-box binding-like 1	0.0004	0.0020	0.90	GO: - Metal ion binding, zinc ion binding - Regulation of transcription, DNA-dependent - Integral to membrane, nucleus
P2RY13	Purinergic receptor P2Y, G-protein coupled, 13	0.0001	0.0020	0.59	GO: - G-protein coupled receptor activity - G-protein coupled receptor protein signalling pathway - Integral to membrane, endoplasmic reticulum
PAK4	p21(CDKN1A)-activated kinase 4	0.0006	0.0020	0.94	Golgi apparatus. Protein transport. Regulation of actin cytoskeleton. GO: - Protein serine/threonine kinase activity, nucleotide binding - Protein amino acid phosphorylation - Golgi apparatus
PEX11G	Peroxisomal biogenesis factor 11 gamma	0.0003	0.0020	0.95	GO: - Peroxisome fission - Integral to membrane

(continued on next page)

Table 1 (*continued*)

Gene symbol	Genes description	Parametric *p*-value	Permutation *p*-value	Intensities ratio (AT/BT)	Function summary (Goterms or/and SP_PIR _KEYWORDS)
POLR3B	Polymerase (RNA) III (DNA-directed) polypeptide B	0.0004	0.0039	0.91	Purine and pyrimidine metabolism. HIV-1 Tat up-regulates the transcription by RNA polymerase III. GO: - Metal ion binding, zinc ion binding, ribonucleoside binding - Transcription - Nucleus
PRAF2	PRA1 domain family, member 2	0.0002	0.0020	1.10	Golgi apparatus. Protein transport. GO: -L-glutamate transport -Endosome, integral to membrane
SLC25A25	Solute carrier family 25 (mitochondrial carrier; phosphate carrier), member 25	0.0005	0.0020	0.72	GO: - Calcium ion binding - Transport - Integral to membrane, mitochondrial inner membrane
SPATA5L1	Spermatogenesis associated 5-like 1	0.0002	0.0020	1.14	GO: - Nucleotide binding, nucleoside-triphosphatase activity
TBC1D14	TBC1 domain family, member 14	0.0005	0.0020	0.83	GO: - GTPase activator activity - Regulation of Rab GTPase activity
TERF1	Telomeric repeat binding factor (NIMA-interacting) 1	0.0003	0.0020	1.14	Component of the telomere nucleoprotein complex, inhibitor of telomerase. GO: - Negative regulation of telomerase activity - Chromosome, nucleus
UTS2	Urotensin 2	0.0001	0.0020	1.08	Highly potent vasoconstrictor. GO: - Hormone activity - Regulation of blood pressure, muscle contraction, synaptic transmission - Extracellular region
VASH1	Vasohibin 1	0.0003	0.0020	0.90	Angiogenesis inhibitor. GO: - Negative regulation of angiogenesis, negative regulation of blood vessel endothelial cell migration - Endoplasmic reticulum, extracellular region
WNT10B	Wingless-type MMTV integration site family, member 10B	0.0001	0.0020	1.07	Adipogenesis. GO: - Wnt receptor signalling pathway, calcium modulating pathway, multicellular organismal development - Extracellular region
ZFP106	Zinc finger protein 106 homolog	0.0001	0.0020	0.85	GO: - Metal ion binding, zinc ion binding - Insulin receptor signalling pathway
ZNF438	Zinc finger protein 438	0.0004	0.0020	0.85	GO: - Metal ion binding, zinc ion binding - Regulation of transcription

Annotation and gene expression information for the 36 candidate genes selected as differentially expressed in PBMC of healthy individuals after low-dose ritonavir treatment. BT: before treatment, AT: after treatment. AT/BT is the intensity ratio between the two states. SP_PIR_KEYWORDS: Protein Information Resource (http://pir.georgetown.edu/) and Swissprot (http://www.expasy.ch/sprot/). Keywords retrieved with DAVID online tool (http://david.abcc.ncifcrf.gov/home.jsp). GOterms: gene ontology terms.

Table 2
Functional class scoring analysis following ritonavir treatment of PBMC gene.

GO category	GO term	GO description	Number of genes	LS permutation *p*-value	KS permutation *p*-value
31497	BP	Chromatin assembly	70	1.00E-05	6.30E-04
16055	BP	Wnt receptor signalling pathway	55	2.12E-03	4.50E-02
17038	BP	Protein import	77	2.13E-03	1.24E-03
7031	BP	Peroxisome organisation and biogenesis	17	2.14E-03	1.20E-01
6471	BP	Protein amino acid ADP-ribosylation	29	2.52E-03	2.34E-03
9126	BP	Purine nucleoside monophosphate metabolic process	15	4.51E-03	3.20E-02
42440	BP	Pigment metabolic process	24	6.70E-03	3.55E-03
7046	BP	Ribosome biogenesis and assembly	13	7.01E-03	1.32E-03
51049	BP	Regulation of transport	41	1.01E-02	4.66E-03
6606	BP	Protein import into nucleus	64	1.49E-02	3.32E-03
16126	BP	Sterol biosynthetic process	26	1.95E-02	1.39E-03
51345	BP	Positive regulation of hydrolase activity	32	3.55E-02	2.17E-03
9311	BP	Oligosaccharide metabolic process	11	3.60E-02	2.33E-03
51223	BP	Regulation of protein transport	19	1.45E-01	3.52E-03
43241	BP	Protein complex disassembly	16	1.46E-01	2.98E-03
3899	MF	DNA-directed RNA polymerase activity	40	1.00E-05	1.00E-05
3950	MF	NAD + ADP-ribosyltransferase activity	25	2.66E-03	9.69E-03
4726	MF	Non-membrane spanning protein tyrosine phosphatase activity	7	3.23E-03	2.35E-01
16857	MF	Racemase and epimerase activity\, acting on carbohydrates and derivatives	6	4.37E-03	5.14E-02
8094	MF	DNA-dependent ATPase activity	35	5.73E-02	2.31E-03
786	CC	Nucleosome	47	1.00E-05	1.00E-05
44439	CC	Peroxisomal part	23	1.76E-03	2.35E-02
228	CC	Nuclear chromosome	48	1.91E-03	1.80E-02
30880	CC	RNA polymerase complex	25	3.49E-03	6.64E-03
43596	CC	Nuclear replication fork	9	4.09E-03	3.23E-03
30027	CC	Lamellipodium	12	2.40E-02	3.44E-03

Gene ontology classes that are differentially expressed before and after ritonavir treatment were evaluated using a functional class scoring analysis (27). For each gene in a GO class, the *p*-value for comparing pre versus post treatment samples was computed. The set of *p*-values for a class was summarised by two summary statistics:

• LS = average log *p*-values for the genes in that class.
• KS = Kolmogorov–Smirnov statistic computed on the *p*-values for the genes in that class.

Twenty six gene ontology classes were shown to be significantly modified following low-dose ritonavir treatment of volunteers PBMC. It is of interest to observe that certain functional classes of genes, such as sterol biosynthesis process (26 genes), and oligosaccharides metabolic process (11 genes), are significantly affected in PBMC following ritonavir treatment. Abbreviations: CC = Cellular Component, MF = Molecular Function, BP = Biological Process.

genes in PBMC, respectively 62, 219, 55 for Random-variance *t*-test, SAM and ANOVA, and their intersection showed a total of 36 candidate genes (Table 1). Five of these genes were up-regulated and 31 were down-regulated in PBMC following ritonavir treatment. It should be noted that 4 of these genes (*ANKRD17*, *DUSP1*, *ERCC1*, *MAP3K6*) are implicated in stress response, 2 (*NCEH1*, *ACSS2*) in lipid metabolism, 4 (*ACSS2*, *AP1M1*, *PAK4*, *PRAF2*) are functionally linked with the Golgi apparatus, and 3 (*ETV6*, *UTS2, VASH1*) are associated with the vascular network. Finally, 3 genes (*NCEH1*, *P2RY13* and *VASH1*) are functionally implicated in the endoplasmic reticulum. The functions of the remaining 23 genes are shown in Table 1.

Functional class scoring

Functional class scoring analysis shows 26 Gene Ontology classes that are significantly altered (p-value<0.005). A break up of these 26 classes shows that 15 are biological processes, 5 are molecular functions and 6 are cellular components (Table 2). The biological process, "chromatin assembly", is observed to be significantly affected and show 27 histone genes that are significantly up-regulated following ritonavir treatment (Table 2). Moreover, histone gene up-regulation was also represented in the cellular component "nucleosome". DNA-directed RNA polymerase activity seems to deregulated molecular processes that seem related. *DUSP1* (ratio of 0.73, p-value = 5E-04) and *KLHDC3* (ratio AT/BT = 0.85, p-value = 8E-05) are the top scoring genes using this functional approach and are implicated respectively in the molecular function "non-membrane spanning protein tyrosine phosphatase activity" and in cellular component "nuclear chromatin" (Fig. 1).

Selection of genes for further analysis by quantitative real time PCR (Q-PCR)

Several lines of evidence have drawn our attention to 2 candidate genes, namely dual specificity phosphatase 1 (*DUSP1*), and Kelch domain containing 3 (*KLHDC3*). Indeed, firstly these 2 genes belong to the list of 36 candidate genes. Secondly, DUSP1 (ratio of 0.73) and KLHDC3 (ratio AT/BT = 0.85) are the top scoring genes using the functional scoring approach. Moreover, 2 other genes, neutral cholesterol ester hydrolase 1 (*NCEH1*) and acyl-CoA synthetase short-chain family member 2 (*ACSS2*), belonging to the lipid metabolism and related pathways and previously cited to be affected by ritonavir in human and murine hepatocytes, were also selected [7,8]. Q-PCR performed on 20 healthy individuals taking part in this study confirm that expression levels of all four candidate genes are significantly down-regulated for 100 mg of ritonavir given once daily (Fig. 1A). Similar gene down-regulation results are observed when 100 mg of ritonavir is given twice daily for *DUSP1*, *KLHDC3* and *ACSS2* genes. Results for *NCEH1* gene shows the same tendency with a p-value of 0.09 (Fig. 1B). The Q-PCR results validate the data obtained using microarrays for the 4 genes.

Pathway analysis

Cytoscape (http://www.cytoscape.org/) software programme was used to investigate links between the four selected genes *ACSS2*, *NCEH1*, *DUSP1* and *KLHDC3* genes. An intermediate gene that link *DUSP1* and *KLHDC3* has been found. Indeed, *DUSP1* is linked to *SKP2* and *CUL1* [11]. Moreover, *CUL1* is linked on the one hand to *MCC* and *CUL2* [12] and on the other to *CAND1* [13,14] which itself is linked to *CUL2* [13,15]. Finally, *KLHDC3* is linked to *CUL2* via *DLG3* [12] (Fig. 2).

Discussion

This study shows for the first time a significant effect of low-dose ritonavir on the modulation of the expression of genes in PBMC of healthy volunteers. Several lines of evidence are presented to show the effects of ritonavir on circulating PBMC: (1) thirty six candidate genes are shown to be significantly modulated by ritonavir. Indeed, stress response, nucleic acid binding, lipid metabolism, Golgi apparatus and vascular network genes present among the 36 candidates are affected by ritonavir. (2) Four genes out of these 36

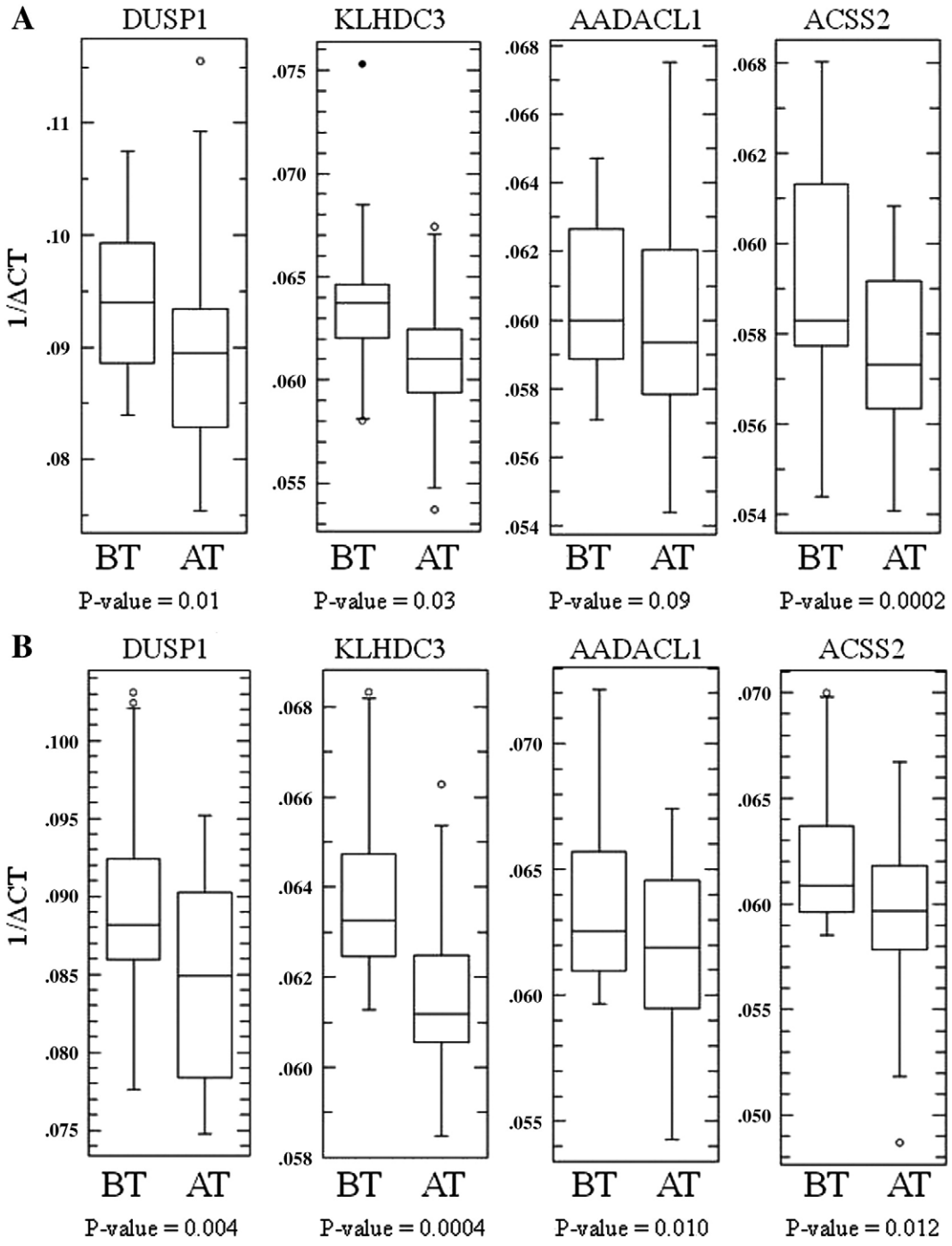

Fig. 1. Q-PCR validation of *DUSP1*, *KLHDC*, *NCEH1* and *ACSS2* genes in PBMC isolated from healthy volunteers before treatment (BT) and after treatment (AT) with low-dose ritonavir. Boxplot of Q-PCR results at BT and AT using total RNA extracted from PBMC from 20 volunteers (p-value<0.05, Student paired t-test). A: group receiving 100 mg of ritonavir once daily and B: the group receiving 100 mg of ritonavir twice daily.

genes, *ACSS2*, *NCEH1*, *DUSP1*, and *KLHDC3*, were shown by Q-PCR in 20 healthy individuals to be significantly down-regulated by ritonavir. (3) Functional class scoring analysis shows 26 Gene Ontology classes that are significantly altered and that ritonavir significantly up-regulates histone families.

In this study, ritonavir is observed to significantly down-regulate stress related gene families such as dual specificity phosphatase 1 (*DUSP1*), excision repair cross-complementing rodent repair deficiency, complementation group 1 (*ERCC1*), *ANKRD17* (ankyrin repeat domain 17), and mitogen-activated protein kinase kinase kinase 6 (*MAP3K6*) (Table 1). It should be noted that previous work equally identified stress related genes in murine adipocytes to be affected following ritonavir treatment [7]. Three genes (*ETV6*, *UTS2*, and *VASH1*) are associated with the vascular network. *ETV6* is known implicated in haematopoiesis and maintenance of the developing vascular network, *UTS2* is a highly potent vasoconstrictor and finally *VASH1* acts as a negative regulation of angiogenesis. Four genes, *AP1M1*, *ACSS2*, *PAK4*, *PRAF2* affected by ritonavir are functionally linked with the Golgi apparatus. *AP1M1* gene is part of *AP-1* complex located at the Golgi vesicle and involved in endocytosis and Golgi

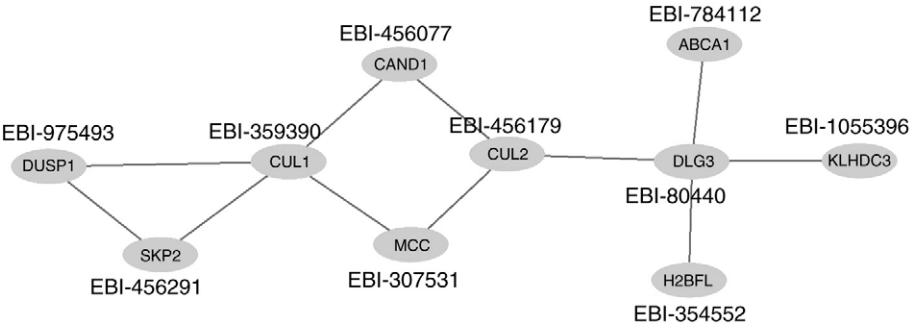

Fig. 2. Genes linking *DUSP1* gene and *KLHDC3*. *DUSP1* and *KLHDC3* genes are linked through a number of intermediary genes that include *CUL1*, *MCC*, *CUL2*, *DLG3* and *CAND1*. Please note that *CUL1* and *CUL2* are connected either via *CAND1* or *MCC*. Moreover, *DUSP1* is connected to *CUL1* and *SKP2*. It is of interest to see that *DLG3* is linked to both *ABCA1* and *HIST1H2BC*. These molecules are all part of molecular complexes or are in direct physical interaction. The evidences of the associations were either produced by coimmunoprecipitation, X-ray crystallography, affinity chromatography technology, peptide array or enzymatic study. The IntAct database identification number is indicated for each gene of the pathway.

processing. Some authors suggested that proper post-Golgi routing of HIV Env protein depends on its recruitment of *AP-1* [16]. Down-regulation of *AP-1* could conceivably inhibit endocytosis of HIV. POLR3B is also known to interact with HIV proteins [17]. *POLR3B* is used by HIV-1 Tat protein to up-regulate viral transcription [18].

Lipid metabolism and related pathways have been reported to be modulated by ritonavir treatment in murine adipocytes [7,8,10] and in human hepatocytes [8]. In this study, lipids were observed to be affected by the ritonavir treatment. Indeed, high-density lipoprotein (HDL) were shown to be decreased by ritonavir 100 mg once daily (6%, $p=0.01$) or 100 mg twice daily (10%, $p=0.001$). Triglyceride levels were observed to increase (32%, $p=0.044$) following ritonavir (100 mg twice daily) [6]. Genes, neutral cholesterol ester hydrolase 1 (*NCEH1*) and acyl-CoA synthetase short-chain family member 2 (*ACSS2*), that belong to the lipid metabolism and related pathways, which include cholesterol and fatty acid biosynthesis are down-regulated in PBMC. The *NCEH1* gene, also known as *KIAA1363* and *NCEH1* (neutral cholesterol ester hydrolase 1), is a central node kin and an ether lipid signalling network that bridges platelet-activating factor and lysophosphatidic acid [19]. It should be noted that *NCEH1* gene has been presented as potential therapeutic target for the prevention of atherosclerosis. Indeed, RNA silencing of *NCEH1* decreases neutral cholesterol ester hydrolase activity at least by 50% whereas over expression of *NCEH1* gene inhibits the cholesterol ester formation in macrophages. In our study, it is conceivable that *NCEH1* down-regulation, following ritonavir treatment, increases the risk of atherosclerosis [20].

The *ACSS2* gene is implicated in various pathways including lipid biosynthetic process, glycolysis/gluconeogenesis pathways and biological oxidation via the reduction of carboxylate cycle. *ACSS2* encodes a cytosolic enzyme that catalyses the activation of acetate for use in lipid synthesis and energy generation. Expression of this gene is regulated by sterol regulatory element-binding proteins, transcription factors that activate genes required for the synthesis of cholesterol and unsaturated fatty acids. Thus, this gene may act at the interface between lipid, glucose and oxidative stress metabolisms (http://www.ncbi.nlm.nih.gov/sites/entrez?db=gene). *ACSS2* and *NCEH1* activities are held within the endoplasmic reticulum, a cellular component that has been previously implicated in lipid disorders associated with ritonavir treatment [7,8].

Previous studies performed on human hepatocytes and murine adipocytes have reported an effect of ritonavir on the endoplasmic reticulum and ER stress response of these cells [7,8]. Interestingly, our results show 3 genes (*NCEH1*, *P2RY13*, *VASH1*), implicated in the endoplasmic reticulum, to be affected by ritonavir. Moreover, an oxidative stress response is shown through the *ERCC1* and *DUSP1* genes. Adler-Wales et al. in line with the current results also reported the implication of oxidative stress after ritonavir treatment [5]. The proteasome following ritonavir treatment is described by Lum et al. to be up-regulated in rat liver and down-regulated in human hepatocytes as observed by Parker et al. [8,10]. The current study does not observe any modulation of the proteosome in PBMC following ritonavir treatment.

Dual specificity phosphatase 1 (*DUSP1*) has very recently been shown to play a major role in inflammation and atherosclerosis [21]. Indeed, Zakkar et al. have demonstrated that *DUSP1* has an anti-inflammatory effect by suppressing *p38* and *MAPK8*. Induction of *DUSP1* appears to be essential in protecting atherosclerosis regions. It is of interest to note that *DUSP1*-deficient macrophages showed selectively prolonged activation of *MAPK14* and increased cytokine production. Gene silencing of *DUSP1* restored *VCAM1* expression, a well known marker of atherosclerosis [21]. One should note that there is a certain amount of controversy on the role of *DUSP1* in atherosclerosis. Indeed, Kang et al., reported that *DUSP1* was one of the two most cited genes (the other one being FOS: v-fos FBJ murine osteosarcoma viral oncogene homolog) that are up-regulated in patients with atherosclerosis compared to controls [22]. In the current study, *DUSP1* is significantly down-regulated in PBMCs of healthy volunteers treated with low-dose ritonavir. Down-regulation of *DUSP1* by low-dose ritonavir may conceivably lower the protection of certain sites that are resistant to atherosclerosis.

The other gene that is down-regulated by low-dose ritonavir in PBMC is Kelch domain containing 3 (*KLHDC3*), about which little is currently known. The protein encoded by this gene, bears six repeated Kelch motifs, and is involved in meiotic recombination. Moreover, this protein appears to be involved in V (D)J recombination and to be expressed specifically in the testis [23]. A homolog of *KLHDC3*, *Drosophila* ring canal Kelch protein, is related to galactose oxidase, an enzyme that cleaves galactose [24]. *DUSP1* and *KLHDC3* genes are linked through a number of intermediary genes (Fig. 2). One of these intermediary linking genes, *CUL2*, is required for the activity of vasculogenesis and hypoxia-inducible factor [25,26]. The other, ATP-binding cassette (*ABC*) transporters (*ABCA1*), functions as a cholesterol efflux pump in macrophages. These molecules are all part of molecular complexes or are in direct physical interaction. The evidence of the association was either produced by coimmunoprecipitation, X-ray crystallography, affinity chromatography technology, peptide array or enzymatic study. We expected to see with the down-regulation of *DUSP1* a certain number of genes that are linked with it such as S-phase kinase-associated protein 2 (*SKP2*) or cullin 1 (*CUL1*) to be also differentially expressed. However, we have not observed a differential expression of these genes. It is conceivable that 14 days of modulation by low-dose ritonavir (100 mg twice daily) is not sufficient to affect *DUSP1* related pathways.

Functional class scoring is based on gene ontology, a controlled and organised vocabulary that describes molecular function, biological process and cellular component of genes products [27,28].

Detailed analysis of affected functional classes (cellular component, molecular function and biological process) is an alternative powerful way to search for candidate genes affected by low-dose ritonavir in circulating volunteer's PBMC. In our experiments, the nucleosome class (containing a total of 47 genes) is significantly affected by low-dose ritonavir. The nucleosome class and nuclear chromatin class are part of the chromatin class (Fig. 1). In the nuclear chromatin class the most significantly affected genes is *KLHDC3* (see Table 2). It is after this observation that we selected the *KLHDC3* gene as a candidate to be tested by Q-PCR.

In conclusion, our investigation on PBMC gene expression, following low-dose ritonavir treatment in healthy donors, shows a significant change in the expression of 36 genes.

To our knowledge this is the only study performed with healthy volunteers that shows for the first time the effect of low-dose ritonavir on gene expression and biological functions in PBMC that may potentially be implicated in inducing metabolic abnormalities and cardiovascular disease. Lower expression levels of *DUSP1*, a gene known to play a critical role in preventing inflammation and atherosclerosis, and *NCEH1*, a gene critically involved in ether lipid signalling network that bridges platelet-activating factor and lysophosphatidic acid, may be some of the factors related to Ritonavir's adverse effects. Such a study provides a powerful combination of tools, using circulating blood cells in tandem with microarrays and Q-PCR, to investigate the secondary effects of ritonavir on treated patients. Generated data obtained by investigating the gene expression levels of circulating PBMC may greatly help in identifying critical genes implicated in the side effects of ritonavir.

Material and methods

Subjects

Male ($n = 10$) and female ($n = 10$) healthy volunteers between 18 and 45 years of age (age matched) were enrolled in this study after giving fully informed and written consent. Subjects were excluded if they had: (1) a history of cigarette smoking or cardiovascular disease, (2) any active clinically significant disease, and (3) been taking any medication or herbal remedy up to 14 days before screening.

Study design

In this study, 2 doses of ritonavir (100 mg once or twice daily, commonly used as boosting doses) were investigated [6]. Eligible subjects were randomised into 2 groups (arm1 and arm2). Indeed, subjects in arm 1 received ritonavir 100 mg orally once daily (o.d.) for 14 days (days 1 to 14) followed by a 14 day-washout period (days 14 to 30) and then ritonavir 100 mg twice daily (b.i.d.) for 14 days (days 30 to 43). Subjects in arm 2 received ritonavir 100 mg twice daily for 14 days, followed by a 14 day-washout period and by ritonavir 100 mg once daily. Blood was drawn before and after treatment or washout periods for all the subjects (arm1 and 2). PBMCs samples from 5 males and 5 females following 100 mg twice daily ritonavir treatment (from arm 1 and 2) were used for the microarray study, whereas all the subjects and both doses (ritonavir 100 mg o.d. and b.i.d.) were investigated by Q-PCR. This study was approved by the Riverside Research Ethics Committee, London, UK. The tolerability and safety of ritonavir were evaluated throughout the study.

Processing of blood samples

Peripheral blood mononuclear cells (PBMC) were isolated from 50 mL blood using Ficoll gradient and stored in RNALater at −20 °C until sample extraction.

Microarrays investigations

RNA samples

PBMCs were thoroughly washed in sterile PBS twice to eliminate traces of RNALater. Total RNA was isolated using the RNeasy mini kit (Qiagen, West Sussex, UK) according to the manufacturer's instructions. Total RNA quantity and integrity were assayed using the Nanodrop ND-1000 (Thermoscientific, Wilmington, DE, USA) and the Agilent 2100 Bioanalyzer (Agilent technology, Palo Alto, CA, USA).

Illumina BeadChips

Samples were processed and data acquired by the microarray core facility of Cambridge University (http://www.path.cam.ac.uk/resources/microarray/) using Sentrix HumanRef8 BeadChips. Briefly, labelled cRNA were prepared using the Illumina RNA amplification kit (Ambion, Austin, TX). The twenty cRNA targets were hybridised to Sentrix human Ref 8 BeadChips, which were scanned on an Illumina BeadStation. Image processing and raw data extraction were performed using the Illumina Beadstudio software. MIAME compliant raw data obtained from all 20 microarrays were deposited at EBI, ArrayExpress repository, under accession number E-TABM-642.

Background adjustment, probe filtering and normalisation

Quality control and pre-processing were performed using the R package lumi (http://www.bioconductor.org/packages/2.2/bioc/html/lumi.html).

A total of 14,596 genes passed the filtering process. We used a Detection Score ≥ 0.99 from the Illumina data as our criteria for a gene to be considered expressed. Model-based variance-stabilising transformation [29] and spline normalisation were followed by microarray quality controls. Boxplot of microarray intensities shows equal mean and variance across samples. Moreover, the density plot shows that the distributions of intensities are identical across all samples.

Differential expression analysis

Differential expression analysis was performed using BRB-ArrayTools developed by Dr. Richard Simon and BRB-ArrayTools Development Team (http://linus.nci.nih.gov/BRB-ArrayTools.html). We identified genes that were differentially expressed among the two classes using a random-variance *t*-test for paired samples [30]. Genes were considered significantly altered if their *p*-value was less than 0.001. We also performed a global test of whether the expression profiles differed between the classes by permuting the labels of which arrays corresponded to which classes (BRB Manual, Sample Statistical Methods Descriptions). Significance Analysis of Microarrays (SAM) was used with a target proportion of false discoveries of 0.15. Analysis of variance (ANOVA) for Mixed Effects Model was used to select genes that are differentially expressed by the factor "treatment" and not by the factor "gender".

Functional class scoring

The functional class scoring analysis for Gene Ontology (GO) classes was performed as described by Palvidis et al. [31] and using BRB-ArrayTools. This approach provides a list of differentially expressed gene ontology classes between before-treatment and after-treatment samples. Functional class scoring analysis evaluates GO categories that are differentially expressed among different phenotype classes 1. It demonstrates an improved technique for identifying differentially expressed gene classes than traditional over-representation analysis.

For each GO group a number of N genes representing the group on the microarray, the statistical significance pi value for each gene *i* in the group is calculated, that reflects the differential expression among classes. Two statistics; the Fisher (LS) statistic and the Kolmogorov–

Smirnov (KS) statistic have been computed for each GO group that summarised the *p*-values for genes in the group. The selection of *N* random genes and *p*-value summarisation are repeated 100,000 times to obtain a distribution of the statistics. Then, the LS (KS) permutation *p*-value is defined as the proportion of selections for each GO category, for which the LS (KS) statistic has a value larger than the LS (KS) statistics computed for the GO category with original gene list. A GO category is selected as differentially expressed if its corresponding LS or KS re-sampling *p*-value is below the threshold specified by the user (default is 0.005) (BRB Manual, Sample Statistical Methods Descriptions).

Pathway analysis

Construction of biological pathway was performed using Cytoscape software package available at http://cytoscape.org/. Cytoscape is an open source bioinformatics software that permit the visualisation of biological pathways integrating public databases and gene expression [32].

Real time quantitative PCR (Q-PCR)

Microarray differentially expressed gene results (*DUSP1*, *KLHDC*, *NCEH1* and *ACSS2*) were validated by Q-PCR using TaqMan® assays (Applied Biosystems). Each amplification was run in duplicates, following retro-transcription of 100 ng/assay of total RNA isolated from 20 healthy subjects. Data were normalised using 18S rRNA. Q-PCR TaqMan® probes were selected to be as similar as possible to those present on Illumina microarrays.

Statistical analysis for real time Q-PCR

Paired Student *t*-test was performed and a difference between groups of patients before and after treatment was considered significant when $p<0.05$. The analyses were performed separately for the group receiving 100 mg of ritonavir once daily and the group receiving 100 mg of ritonavir twice daily.

Acknowledgments

This work was supported by a grant from the St. Stephen's AIDS Trust, London, UK. John L. McGregor would like to warmly thank INSERM for a grant.

References

[1] E. De Clercq, Anti-HIV drugs: 25 compounds approved within 25 years after the discovery of HIV, Int. J. Antimicrob. Agents (2008).
[2] G. Gatti, et al., The relationship between ritonavir plasma levels and side-effects: implications for therapeutic drug monitoring, AIDS 13 (15) (1999) 2083–2089.
[3] B. Gazzard, et al., British HIV Association (BHIVA) guidelines for the treatment of HIV-infected adults with antiretroviral therapy (2006), HIV Med. 7 (8) (2006) 487–503.
[4] J.S. Currier, et al., Coronary heart disease in HIV-infected individuals, J. Acquir. Immune. Defic. Syndr. 33 (4) (2003) 506–512.
[5] S.D. Shafran, L.D. Mashinter, S.E. Roberts, The effect of low-dose ritonavir monotherapy on fasting serum lipid concentrations, HIV Med 6 (6) (2005) 421–425.
[6] S. Collot-Teixeira, et al., Impact of Different Low-Dose Ritonavir Regimens on Lipids, CD36, and Adipophilin Expression, Clin. Pharmacol. Ther. (2008).
[7] D.C. Adler-Wailes, et al., Effects of ritonavir on adipocyte gene expression: evidence for a stress-related response, Obesity (Silver Spring) 16 (10) (2008) 2379–2387.
[8] R.A. Parker, et al., Endoplasmic reticulum stress links dyslipidemia to inhibition of proteasome activity and glucose transport by HIV protease inhibitors, Mol. Pharmacol. 67 (6) (2005) 1909–1919.
[9] A.P. Malizia, et al., HIV1 protease inhibitors selectively induce inflammatory chemokine expression in primary human osteoblasts, Antiviral Res. 74 (1) (2007) 72–76.
[10] P.Y. Lum, et al., Gene expression profiling of rat liver reveals a mechanistic basis for ritonavir-induced hyperlipidemia, Genomics 90 (4) (2007) 464–473.
[11] Y.W. Lin, J.L. Yang, Cooperation of ERK and SCFSkp2 for MKP-1 destruction provides a positive feedback regulation of proliferating signaling, J. Biol. Chem. 281 (2) (2006) 915–926.
[12] R.M. Ewing, et al., Large-scale mapping of human protein–protein interactions by mass spectrometry, Mol. Syst. Biol. 3 (2007) 89.
[13] K.W. Min, et al., TIP120A associates with cullins and modulates ubiquitin ligase activity, J. Biol. Chem. 278 (18) (2003) 15905–15910.
[14] S.J. Goldenberg, et al., Structure of the Cand1–Cul1–Roc1 complex reveals regulatory mechanisms for the assembly of the multisubunit cullin-dependent ubiquitin ligases, Cell 119 (4) (2004) 517–528.
[15] J. Zheng, et al., CAND1 binds to unneddylated CUL1 and regulates the formation of SCF ubiquitin E3 ligase complex, Mol. Cell. 10 (6) (2002) 1519–1526.
[16] S. Wyss, et al., The highly conserved C-terminal dileucine motif in the cytosolic domain of the human immunodeficiency virus type 1 envelope glycoprotein is critical for its association with the AP-1 clathrin adaptor [correction of adapter], J. Virol. 75 (6) (2001) 2982–2992.
[17] W. Fu, et al., Human immunodeficiency virus type 1, human protein interaction database at NCBI, Nucleic Acids Res. (2008).
[18] K.L. Jang, M.K. Collins, D.S. Latchman, The human immunodeficiency virus tat protein increases the transcription of human Alu repeated sequences by increasing the activity of the cellular transcription factor TFIIIC, J. Acquir. Immune. Defic. Syndr. 5 (11) (1992) 1142–1147.
[19] K.P. Chiang, et al., An enzyme that regulates ether lipid signaling pathways in cancer annotated by multidimensional profiling, Chem. Biol. 13 (10) (2006) 1041–1050.
[20] H. Okazaki, et al., Identification of neutral cholesterol ester hydrolase, a key enzyme removing cholesterol from macrophages, J. Biol. Chem. 283 (48) (2008) 33357–33364.
[21] M. Zakkar, et al., Increased endothelial mitogen-activated protein kinase phosphatase-1 expression suppresses proinflammatory activation at sites that are resistant to atherosclerosis, Circ. Res. 103 (7) (2008) 726–732.
[22] J.G. Kang, et al., Genomic analysis of circulating cells: a window into atherosclerosis, Trends Cardiovasc. Med. 16 (5) (2006) 163–168.
[23] Y. Ohinata, S. Sutou, Y. Mitsui, A novel testis-specific RAG2-like protein Peas: its expression in pachytene spermatocyte cytoplasm and meiotic chromatin, FEBS Lett. 537 (1–3) (2003) 1–5.
[24] S.F. Altschul, et al., Gapped BLAST and PSI-BLAST: a new generation of protein database search programs, Nucleic Acids Res. 25 (17) (1997) 3389–3402.
[25] Y. Maeda, et al., CUL2 is required for the activity of hypoxia-inducible factor and vasculogenesis, J. Biol. Chem. 283 (23) (2008) 16084–16092.
[26] N. Mahrour, et al., Characterization of Cullin-box sequences that direct recruitment of Cul2–Rbx1 and Cul5–Rbx2 modules to Elongin BC-based ubiquitin ligases, J. Biol. Chem. 283 (12) (2008) 8005–8013.
[27] S. Lewis, M. Ashburner, M.G. Reese, Annotating eukaryote genomes, Curr. Opin. Struct. Biol. 10 (3) (2000) 349–354.
[28] M. Ashburner, et al., Gene ontology: tool for the unification of biology. The Gene Ontology Consortium, Nat. Genet. 25 (1) (2000) 25–29.
[29] S.M. Lin, et al., Model-based variance-stabilizing transformation for Illumina microarray data, Nucleic Acids Res. 36 (2) (2008) e11.
[30] G.W. Wright, R.M. Simon, A random variance model for detection of differential gene expression in small microarray experiments, Bioinformatics 19 (18) (2003) 2448–2455.
[31] P. Pavlidis, D.P. Lewis, W.S. Noble, Exploring gene expression data with class scores, Pac. Symp. Biocomput. (2002) 474–485.
[32] P. Shannon, et al., Cytoscape: a software environment for integrated models of biomolecular interaction networks, Genome Res. 13 (11) (2003) 2498–2504.